

Sticky Rouse Model and Molecular Dynamics Simulation for Dual Polymer Networks

*Jingyu Shao, Nuofei Jiang, Hongdong Zhang, Yuliang Yang and Ping Tang**

State Key Laboratory of Molecular Engineering of Polymers, Department of Macromolecular Science, Fudan University, Shanghai 200433, China

1. The analytical eigenvalue for affine-based dual network model

We consider that the two end beads of the model do not relax, and thus the effective friction coefficient of those is set to be positive infinity, namely $\delta' \rightarrow \infty$ in the modified SRM, represented by the black solid beads in Figure S1b. In addition, we introduce the sticker into the affine network, which has a finite friction coefficient δ , shown by the gray filled beads in Figure S1b. The hollow bead is the normal segment in strands, whose length is $2n + 3$, where the half chain length between the sticker and the end segment is n .

On the basis of Theorem I,¹ the eigen-polynomial of RZ matrix for affine dual network model is $P_Q(x)$, which can be split into two subgraphs Q' and Q^i from the location of sticker with removing or non-removing the closed path passing, as shown in Figure S1b. The eigen-polynomial from graph theory aspect can be written as follows:

$$P_Q(x) = P_{Q'}(x) + \sum_i \eta_i P_{Q^i}(x) \quad (\text{S.1})$$

where $x \equiv 2 - \lambda$, $P_{Q'}$ is the eigen-polynomial of subgraphs by cutting the middle bond, P_{Q^i} is that of subgraphs by removing the closed path passing through the middle bond, η_i is the bond weighting factor showing the connectivity between beads, i represents the number of closed paths, for example, $i=1$ and $P_{Q^1}(x) = P_{Q_1}(x)P_{Q_2}(x)$ in the case of Figure S1b.

However, in the expression of matrix operations instead of graph theory, the determinant of $P_Q(x)$ can be written as the sum of the cofactors of the sticker's row or column of the matrix multiplied by the entries that generate them. By introducing two basic and analytically solvable Tshebyshev polynomials $p_n(x)$ and $\dot{p}_n(x)$, representing the eigen-polynomials of RZ matrix for two kinds linear chains shown in Figure S1a, the eigen-polynomial $P_Q(x)$ can be expressed as a function of the two basic polynomials.¹

$$\begin{aligned}
P_Q(x) &= P_{Q_i}(x)P_{Q_j}(x) - P_{Q_j}(x)P_{Q_i}(x) \\
&= P_{Q_j}(x) \left[(2 - 2\delta + x\delta)P_{Q_i}(x) - 2P_{Q_i}(x) \right] \\
&\stackrel{\delta' \rightarrow \infty}{\approx} (\phi - 2\delta' + x\delta')^2 p_n(x) \left[(2 - 2\delta + x\delta)p_n(x) - 2p_{n-1}(x) \right] \\
&= \delta'^2 (x-2)^2 \Gamma_1 \Gamma_2
\end{aligned} \tag{S.2}$$

As a result, we divide the complex eigen-polynomials of dual network model into the product of two basic eigen-polynomials Γ_1 and Γ_2 . Then calculating the eigenvalues is naturally transformed into finding the solution of the two basic eigen-polynomials. The polynomial $\Gamma_1 = p_n(x)$, whose analytic eigenvalues can be calculated directly as $\lambda_p = 2 - 2\cos(p\pi/(n+1)), (p=1, 2, \dots, n)$. The other polynomial $\Gamma_2 = (2 - 2\delta + x\delta)p_n(x) - 2p_{n-1}(x)$, which has a non-zero minimum eigenvalue reflecting the diffusion motion of stickers. With θ in the weighting factors $x = 2\cos\theta$ tends to zero, we substitute Tshebyshev polynomials into Γ_2 and obtain the minimum eigenvalue with the Taylor expansion of θ .

$$\lambda_s \approx \frac{6}{3n + 3\delta + 3n\delta + 3n^2 + 1} \tag{S.3}$$

Actually, $P_Q(x)$ has another two eigenvalues smaller than λ_s . One is the infinite small eigenvalue of end segment that nearly does not relax, and the other is the only one zero

eigenvalue $\lambda_0 = 0$, corresponding to the translational diffusion of the entire chain. However, the diffusion motion of entire chain has no effect on the rheological properties, and this holds true for any topologies in Rouse model.¹ Polynomials Γ_2 can be further simplified when $\delta \gg 2$,

$$\Gamma_2 = (2 - 2\delta + x\delta) p_n(x) - 2p_{n-1}(x) \stackrel{\delta \gg 2}{\approx} \delta(x-2) p_n(x) \quad (\text{S.4})$$

the general solution in eq (S.4) is consistent with Γ_1 , and the complete polynomials of the entire chain can be obtained.

$$P_Q(x) \stackrel{\delta \gg 2}{\approx} \delta'^2 \delta(x-2)^3 p_n^2(x) \quad (\text{S.5})$$

Finally, the following eigenvalues of the dual network model based on affine deformation can be obtained, which contains $\lambda_0 = 0$, representing the translational diffusion of entire chain, $\lambda_s \approx 0$ for the arched peripheral bead, λ_s and λ_p show the slow diffusion motion of stickers and the Rouse relaxation of strands, where λ_s can reduce to the minimum eigenvalues of homopolymer chains with $\delta = 1$, that is $\lambda_s \approx 2/(n+1)^2$.

2. The analytical eigenvalue for phantom-based dual network model

Based on the affine-based dual network model, we further extend to the phantom-based structure in this section. Since we adopt phantom-based structures, the graph theory can simplify its Zimm matrix based on the symmetry. According to the topological structures and functionality of each segments, the structure of the dual polymer network can be divided into several linear structures according to the proved theorem, and thus we can get the analytic eigen-polynomial of the entire polymer dual networks, shown in Figure S2.¹⁻³ Following Theorem IV, subgraphs can be generally classified into two categories, that is $P_{A(g_m-1)B}(x)$ and $P_{(g-1)B}(x)$, where g_m indicates the maximum generation in the polymer dual network model. The final eigen-polynomial can be drawn out as the product of the eigen-polynomials

of subgraphs:

$$\Gamma_{g_m, \phi}(x) = P_{A(g_m-1)B}(x) P_{(g_m-1)B}^{\phi-1}(x) \prod_{g=1}^{g_m-1} P_{(g-1)B}^{\phi(\phi-2)(\phi-1)^{g_m-g-1}}(x) \quad (\text{S.6})$$

Yang et al have proved the above formula can degenerate into many known solutions in special cases, which has strong universalities.³ For example, eq (S.6) can reduce to linear chain when $\phi = 2$ and reduce to starlike chain when $g_m = 1$, $\phi > 2$. Besides, the degeneracy of each eigen-polynomial can be obtained in eq (S.6), where $P_{A(g_m-1)B}(x)$ is non-degenerated, $P_{(g_m-1)B}(x)$ is $(\phi-1)$ -fold degenerated and $P_{(g-1)B}(x)$ is $[\phi(\phi-2)(\phi-1)^{g_m-g-1}]$ -fold degenerated. The goal of analytical deduction turns to solving two categories of subgraphs.

Figure S3 shows critical subgraphs in detail. The weighting factors of bonds and the beads has been marked, and the specific eigen-polynomial of each subgraph can be calculated by the graph theory like the affine-based dual network model above. The specific eigen-polynomial of several basic subgraph can be ducted from their structure following Theorem I. For example, P_R can be obtained by cutting the bond connecting the sticker, which is written as,

$$P_R = p_n(x) [(2 - 2\delta + x\delta) p_n(x) - 2p_{n-1}(x)] \quad (\text{S.7})$$

where δ is the effective friction coefficient. Similarly, P_S and P_H can be expressed from the same way.

$$P_S(x) = p_n(x) [(2 - 2\delta + x\delta) p_{n-1}(x) - p_{n-2}(x)] - p_{n-1}^2(x) \quad (\text{S.8})$$

$$P_H = p_{n-1}(x) [(2 - 2\delta + x\delta) p_{n-1}(x) - 2p_{n-2}(x)] \quad (\text{S.9})$$

For the subgraph with junction segments, the eigen-polynomial is still calculated within the framework of Theorem I by cutting the bond connecting the junction, which is the functions of P_R , P_H and P_S .

$$P_L = (x + \phi - 2)P_S - P_H \quad (\text{S.10})$$

$$P_P = (x + \phi - 2)P_R - P_S \quad (\text{S.11})$$

For the subgraph with peripheral segments arched in the space, the eigen-polynomial is obtained by cutting the bond connecting the arched bead, and it can be simplified further based on the infinite effective friction coefficient.

$$P_B = (\phi - 2\delta' + x\delta')P_R - P_S \approx (\phi - 2\delta' + x\delta')P_R \quad (\text{S.12})$$

However, the four general subgraphs have obvious translational symmetry, and their analytical eigen-polynomial can be calculated according to Theorem V:

$$P_n(x) = t^n P_n\left(\frac{Z}{t}\right) + (\phi - 1)P_S(x)t^{n-1}P_{n-1}\left(\frac{Z}{t}\right) \quad (\text{S.13})$$

$$P_{L(n)}(x) = P_L(x)t^n P_n\left(\frac{Z}{t}\right) \quad (\text{S.14})$$

$$P_{(n)R}(x) = P_R(x)t^n P_n\left(\frac{Z}{t}\right) \quad (\text{S.15})$$

$$\begin{aligned} P_{L(n)R}(x) &= P_L(x)P_{(n)R} - (\phi - 1)P_S(x)P_{L(n-1)R} \\ &= \frac{1}{\phi - 1} \left[P_P(x)t^{n+1}P_{n+1}\left(\frac{Z}{t}\right) - t^{n+2}P_{n+2}\left(\frac{Z}{t}\right) \right] \end{aligned} \quad (\text{S.16})$$

where $Z(x) = P_P(x) - (\phi - 1)P_S(x)$ and $t = \sqrt{(\phi - 1)(P_R(x)P_L(x) - P_P(x)P_S(x))}$. In our case $P_R(x)P_L(x) - P_P(x)P_S(x) = 1$, and thus $t = \sqrt{\phi - 1}$. With the above four general eigen-polynomials and six basic polynomials, we can go further to derive the eigen-polynomials of the two categories of subgraphs $P_{A(g_m-1)B}(x)$ and $P_{(g-1)B}(x)$:

$$\begin{aligned} P_{A(g_m-1)B}(x) &= (x + \phi - 2)P_{(g_m-1)B}(x) - \phi P_{L(g_m-2)B}(x) \\ &\stackrel{\delta' \rightarrow \infty}{\approx} (x + \phi - 2) \left[(4 - 2\delta' + x\delta')P_{(g_m-1)R}(x) \right] - \phi \left[(4 - 2\delta' + x\delta')P_{L(g_m-2)R}(x) \right] \\ &= (4 - 2\delta' + x\delta') \left[\left((x + \phi - 2)P_R(x) - \frac{\phi}{\phi - 1}P_P(x) \right) t^{g_m-1} p_{(g_m-1)}\left(\frac{Z}{t}\right) + \frac{\phi}{\phi - 1} t^{g_m} p_{(g_m)}\left(\frac{Z}{t}\right) \right] \end{aligned} \quad (\text{S.17})$$

$$\begin{aligned}
P_{(g-1)B}(x) &\stackrel{\delta' \rightarrow \infty}{\approx} (4 - 2\delta' + x\delta') P_{(g-1)R}(x) \\
&= (4 - 2\delta' + x\delta') P_R(x) t^{g-1} p_{g-1}\left(\frac{Z}{t}\right)
\end{aligned} \tag{S.18}$$

the next step is to find the analytic solutions of eq (S.17) and eq (S.18) through known conditions.

2.1 Analytical solutions for $P_{(g-1)B}(x)$

$p_g(Z/t)$ is introduced for dealing with the translational symmetry of subgraphs, which has the same form as the Tshebyshev polynomial with the argument calculated from the eigen-polynomial of the repeating unit. The detail for $p_g(Z/t)$ refer to the work of Yang et al.³ The Z/t can be written as a function of $p_n(x)$:

$$\begin{aligned}
\frac{Z}{t} &= \frac{1}{\sqrt{\phi-1}} \left[(x+\phi-2) p_n(x) \left[(2-2\delta+x\delta) p_n(x) - 2p_{n-1}(x) \right] \right. \\
&\quad \left. - \phi \left[p_n(x) \left[(2-2\delta+x\delta) p_{n-1}(x) - p_{n-2}(x) \right] - p_{n-1}^2(x) \right] \right]
\end{aligned} \tag{S.19}$$

defining $Z/t = 2 \cosh \Phi$, we will have

$$p_g\left(\frac{Z}{t}\right) = \frac{\sinh(g+1)\Phi}{\sinh \Phi} \tag{S.20}$$

substituting eq (S.20) and eq (S.7) into eq (S.18), the following eigen-polynomials for $P_{(g-1)B}(x)$ can be obtained as

$$\begin{aligned}
P_{(g-1)B}(x) &= (4 - 2\delta' + x\delta') p_n(x) \left[(2 - 2\delta + x\delta) p_n(x) - 2p_{n-1}(x) \right] \\
&\quad \cdot t^{g-1} \frac{\sinh(g\Phi)}{\sinh \Phi} \\
&= (4 - 2\delta' + x\delta') t^{g-1} \Gamma'_1 \Gamma'_2 \Gamma'_3
\end{aligned} \tag{S.21}$$

similar to the above results based on the affine deformation, the complex eigen-polynomial is divided into the product of three basic eigen-polynomials Γ'_1 , Γ'_2 and Γ'_3 . So, the analytic solution is also in three parts.

$$\Gamma'_1 = p_n(x) \quad (\text{S.22})$$

$$\Gamma'_2 = (2 - 2\delta + x\delta) p_n(x) - 2p_{n-1}(x) \quad (\text{S.23})$$

$$\Gamma'_3 = \sinh(g\Phi)/\sinh\Phi \quad (\text{S.24})$$

The analytic solution of Γ'_1 is directly obtain as

$$\lambda_p = 2 - 2\cos(p\pi/(n+1)), (p = 1, 2, \dots, n) \quad (\text{S.25})$$

The calculation of non-zero minimum eigenvalue in Γ'_2 is same as the above derivation, that is, substituting $x = 2\cos\theta$ into eq (S.23) and obtaining the non-zero minimum eigenvalue λ_s based on the Taylor expansion of θ , which is the same as eq (S.3). When $\delta \gg 2$, Γ'_2 can be further simplified, and the general solution is consistent with polynomial Γ'_1 .

$$\Gamma'_2 = (2 - 2\delta + x\delta) p_n(x) - 2p_{n-1}(x) \stackrel{\delta \gg 2}{\approx} \delta(x-2) p_n(x) \quad (\text{S.26})$$

$\Gamma'_3 = \sinh(g\Phi)/\sinh\Phi$ only exists in the case of $g > 1$, and the solution of eigenvalue can be obtained directly by $\sinh(g\Phi) = 0$,

$$\Phi = ik\pi/g, (k = 1, 2, \dots, g-1) \quad (\text{S.27})$$

Substituting eq (S.27) into definition $Z/t = 2\cosh\Phi$, we further have

$$\begin{aligned} \frac{Z}{t} &= 2\cosh\left(\frac{ik\pi}{g}\right) \\ &= \frac{1}{\sqrt{\phi-1}} \left[(x+\phi-2) p_n(x) [(2-2\delta+x\delta) p_n(x) - 2p_{n-1}(x)] \right. \\ &\quad \left. - \phi [p_n(x) [(2-2\delta+x\delta) p_{n-1}(x) - p_{n-2}(x)] - p_{n-1}^2(x)] \right] \\ &= 2\cos\frac{k\pi}{g} \end{aligned} \quad (\text{S.28})$$

eq (S.28) contains the effect of translational symmetry on eigenvalues, and the difference of eigenvalues between repeating units lies in $\cos(k\pi/g)$. In the same way, we can obtain $\lambda_{s,k}$ with the Taylor expansion of θ .

$$\lambda_{s,k} \approx \frac{\phi - 2\sqrt{\phi-1} \cos\left(\frac{k\pi}{g}\right)}{2n + 2\phi n + \phi\delta + 2\phi n^2 + \phi n\delta + 2} \quad (\text{S.29})$$

Eq (S.29) also can be further simplified with $\delta \gg 2$,

$$\frac{1}{\sqrt{\phi-1}}(x-2)\delta p_n(x) [\dot{p}_{n+1}(x) + (\phi-1)\dot{p}_n(x)] = 0 \quad (\text{S.30})$$

the analytic expression for the solution of $p_n(x)$ is obtained as the Tshebyshev polynomial, but the $\dot{p}_{n+1}(x) + (\phi-1)\dot{p}_n(x)$ term obviously has no analytic solution, which is only calculated with assumption of large n .

$$\lambda'_p = 2 - 2\cos\left(\frac{(2p-1)\pi}{(2n+1)}\right), (p=1, 2, \dots, n) \quad (\text{S.31})$$

Up to now, we have already obtained all analytical solutions of the subgraph $P_{(g-1)B}(x)$. The general solution contains $(k+2)$ -fold λ_p , k -fold λ'_p , $g-1$ non-zero minimum eigenvalues $\lambda_{s,k}$ for repeated unit in the case of $g > 1$ and λ_s for that of $P_{(0)B}(x)$.

2.2 Analytical solutions for $P_{A(g_m-1)B}(x)$

Subgraph $P_{A(g_m-1)B}(x)$ is a more complex eigen-polynomials, which considers the influence of the mid junction. It is essentially a special case of $P_{(g-1)B}(x)$ and does not have analytical solution intuitively, which need to be simplified further. Assume the maximum generation g_m tends to be infinite, the influence of peripheral unit disappears, and $p_{g_m-1}(Z/t) \approx p_{g_m}(Z/t)$. Substituting the approximate equality into the eq (S.17), we can get its simplest form

$$P_{A(g_m-1)B}(x) = (4 - 2\delta' + x\delta') p_{(g_m)}\left(\frac{Z}{t}\right) \left[\left((x + \phi - 2) P_R(x) - \frac{\phi}{\phi-1} P_P(x) \right) t^{g_m-1} + \frac{\phi}{\phi-1} t^{g_m} \right] \quad (\text{S.32})$$

in this case, the solution of eigen-polynomials is reduced to that of $p_{g_m-1}(Z/t)$.

Similar to the above deviation, the eigenvalues of $p_{g_m-1}(Z/t)$ includes three types. One is the $\lambda_{s,k}$ due to the existence of sticker with the argument of g_m ,

$$\lambda_{s,k} \approx \frac{\phi - 2\sqrt{\phi-1} \cos\left(\frac{k\pi}{g_m}\right)}{2n + 2\phi n + \phi\delta + 2\phi n^2 + \phi n\delta + 2}, (k = 1, 2, \dots, g_m - 1) \quad (\text{S.33})$$

another is the general solution obtained above when $\delta \gg 2$, which has k -fold λ_p and k -fold λ'_p . Moreover, the last solution is the zero eigenvalue that corresponds to the translational diffusion of the entire network.

3. The strand size and MSD simulations for junctions in network

The mean square displacement (MSD) $g_2^j(t)$ is written as

$$g_2^j(t) = \left\langle \left\{ \left[r_j(t) - \mathbf{R}_{c.m.}(t) \right] - \left[r_j(0) - \mathbf{R}_{c.m.}(0) \right] \right\}^2 \right\rangle \quad (\text{S.34})$$

where $r_j(t)$ is the spatial position at time t , and $\mathbf{R}_{c.m.}(t)$ is the center of mass. In the short period, the motion of strands is not constrained by crosslinks, and it will follow Rouse dynamics. However, each junction has a maximum MSD based on the connectivity of the network, which is predicted by Erman et al. with phantom network structure, $g_2^j(t \rightarrow \infty) = (\phi-1)/\phi(\phi-2) \langle R^2(N_s) \rangle$.⁴ In our simulation, we mainly focus on the four-fold networks, and thus we expect $g_2^j(t \rightarrow \infty) = (3/8)R^2(N_s)$, which is solid without the influence of entanglement.

We implement six simulations on one strand length N_s , and consider the mean square end-to-end distance of strands on both the time average and the ensemble average $\langle R^2(N_s) \rangle$, shown in Figure S4a. As expected, $\langle R^2(N_s) \rangle \propto N_s$, which means the strands in networks are Gaussian-like. In turn, we observe Rouse dynamics of strands at short time in Figure S4b. The prediction without entanglements is present as black dotted lines, which is perfectly

consistent with the simulation results. However, the deviation between them becomes significantly large with increased N_s due to the uncrossability of chains, even for the strands smaller than the melt entanglement length $N_e = 35$.⁵ The motion will be retarded extremely when $N_s \gg N_e$ with the increased restrictions on junctions, and their diffusion is expected within the spatial regime of the reptation tube diameter.^{6,7} Thus we have the relation,

$$g_2^j(t \rightarrow \infty)^{-1} = \Delta^{-2} + aN_s^{-1} \quad (\text{S.35})$$

where a is a constant, and it is supposed to be $(\phi-1)/\phi(\phi-2)$ with the assumption of phantom network. The space between junctions become large with increased N_s , allowing the magnitude of fluctuation becomes larger, and Δ^{-2} tends to be zero. However, the MSD asymptotically becomes independent of the strand length when $N_s^{-1} \rightarrow 0$, shown in eq (S.35) and Figure S3c, and the $\Delta^{-2} \approx 0.041$ with the entangled networks. The extrapolation result is almost exactly the same length as the characteristic displacement of the monomers within the tube $20\sigma^2$, which is approximately equal to the $2R_G^2(N_e)$, and the above results are consistent with that of Grest and Kremer, et al.^{5,7}

4. The deduction of analytic linear relaxation modulus

The subgraphs contributions for the overall linear relaxation modulus can be measured by its segments number density $\alpha(\phi, g)$. For the dual polymer network with the maximum generation g_m , the total segments can be calculated with $N_s = 2n + 2$, where n represents the half strand length divided by stickers in our model picture. The subgraph eigen polynomial $P_{(g-1)B}(x)$ has the number of segments $N_{g-1} = \phi(\phi-2)g(2n+2)(\phi-1)^{g_m-g-1}$ with the segments number density $\alpha(\phi, g) \approx (\phi-2)^2 \left[g / (\phi-1)^{g+1} \right]$, where $x \equiv 2 - \lambda$ represents weighting factors of segments. However, the segments number density of $P_{(g_m-1)B}(x)$ and

$P_{A(g_m-1)B}(x)$ becomes zero with $g \rightarrow \infty$, and thus we neglect the influence of those two subgraphs for simplifying calculations. The general expression of the linear relaxation modulus can be written as the function of eigenvalues,

$$G(\phi, t) = \sum_{g=1}^{g_m} \alpha(\phi, g) \left(\frac{\rho}{(2n+2)g} \right) \left\{ \sum_{p=g+1}^{g(2n+2)} \exp(-2\lambda_p t) + \sum_{k=1}^{g-1} \exp(-2\lambda_{s,k} t) + \exp(-2\lambda_s t) \right\} \quad (\text{S.36})$$

in our model, the relaxation time of the sticker is much longer than that of the subchains, that is, the effective friction coefficient δ is large. Thus, the minimum eigenvalues λ_s or $\lambda_{s,k}$ have a simplified form.

$$\lambda_s \approx \frac{2}{n\delta} \quad (\text{S.37})$$

$$\lambda_{s,k} \approx \frac{\phi - 2\sqrt{\phi-1} \cos\left(\frac{k\pi}{g}\right)}{\phi n\delta} = \frac{\phi - 2\sqrt{\phi-1}}{\phi n\delta} + \frac{4\sqrt{\phi-1}}{\phi n\delta} \sin^2\left(\frac{k\pi}{2g}\right) \quad (\text{S.38})$$

However, each subgraph owns the translational symmetry with g periods, and each periodic strand owns $2n$ segments separated by one sticker. According to the simplified method of graph theory, the relaxation behaviors of half strands in one period are different and can be split apart as λ_p term and λ'_p term, that is, λ_p with $(g+1)$ -fold and λ'_p with g -fold. We substitute analytic eigenvalues calculated above into eq. (S.36), and obtain the further linear relaxation modulus of dual polymer network.

$$\begin{aligned} G(\phi, t) &= \sum_{g=1}^{g_{\max}} \alpha(\phi, g) \left(\frac{\rho}{(2n+2)g} \right) \left\{ (g+1) \sum_{p=1}^n \exp\left(-8 \sin^2\left(\frac{p\pi}{2(n+1)}\right) t\right) + (g-1) \sum_{p=1}^n \exp\left(-8 \sin^2\left(\frac{(2p-1)\pi}{2(2n+1)}\right) t\right) \right. \\ &\quad \left. + \sum_{k=1}^{g-1} \exp\left[-2 \left(\frac{\phi - 2\sqrt{\phi-1}}{\phi n\delta} + \frac{4\sqrt{\phi-1}}{\phi n\delta} \sin^2\left(\frac{k\pi}{2g}\right) \right) t\right] + \exp\left(-\frac{4}{n\delta} t\right) \right\} \\ &= \sum_{g=1}^{g_{\max}} \alpha(\phi, g) \left(\frac{\rho}{(2n+2)g} \right) \left\{ (g+1) \sum_{p=1}^n \exp\left(-8 \left(\frac{p^2 \pi^2}{4(n+1)^2} \right) t\right) + (g-1) \sum_{p=1}^n \exp\left(-8 \left(\frac{(2p-1)^2 \pi^2}{4(2n+1)^2} \right) t\right) \right. \\ &\quad \left. + \sum_{k=1}^{g-1} \left\{ \exp\left[-\frac{8\sqrt{\phi-1}}{\phi n\delta} \left(\frac{k^2 \pi^2}{4g^2} \right) t\right] \exp\left(-2 \frac{\phi - 2\sqrt{\phi-1}}{\phi n\delta} t\right) \right\} + \exp\left(-\frac{4}{n\delta} t\right) \right\} \end{aligned} \quad (\text{S.39})$$

We should note that the information of translational symmetry disappears with $g = 1$, and eq (S.39) is further reduced by Gauss integration with assumption of large g and n .

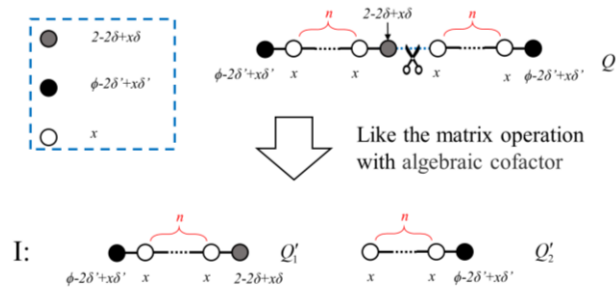
$$\begin{aligned}
G(\phi, t) &= \sum_{g=2}^{g_{\max}} \alpha(\phi, g) \left(\frac{\rho}{(2n+2)g} \right) \left\{ \frac{(g+1)}{2\sqrt{2}} \left(\frac{(n+1)^2}{\pi t} \right)^{1/2} + \frac{(g-1)}{2\sqrt{2}} \left(\frac{(2n+1)^2}{4\pi t} \right)^{1/2} \right. \\
&\quad \left. + \frac{(g-1)}{2\sqrt{2}} \left(\frac{\phi n \delta}{\sqrt{\phi-1}\pi t} \right)^{1/2} \exp\left(-2 \frac{\phi-2\sqrt{\phi-1}}{\phi n \delta} t\right) + \exp\left(-\frac{4}{n\delta} t\right) \right\} \\
&\quad + \frac{(\phi-2)^2}{(\phi-1)^2} \frac{\rho}{2n+2} \left\{ \left(\frac{(n+1)^2}{2\pi t} \right)^{1/2} + \exp\left(-\frac{4}{n\delta} t\right) \right\} \\
&= \sum_{g=2}^{g_{\max}} \alpha(\phi, g) \left(\frac{\rho}{(2n+2)g} \right) \left\{ \frac{(g+1)}{2\sqrt{2}} \left(\frac{\pi\tau_R}{t} \right)^{1/2} + \frac{(g-1)}{2\sqrt{2}} \left(\frac{\pi\tau'_R}{t} \right)^{1/2} + \frac{(g-1)}{2\sqrt{2}} \left(\frac{\pi\tau_{sb}}{t} \right)^{1/2} \exp\left(-\frac{2t}{\tau'_{sb}}\right) \right\} \\
&\quad + \frac{(\phi-2)^2}{(\phi-1)^2} \frac{\rho}{2n+2} \left\{ \left(\frac{\pi\tau_R}{2t} \right)^{1/2} + \exp\left(-\frac{4}{n\delta} t\right) \right\} \\
&= \frac{1}{2\sqrt{2}} \left(1 - \frac{(\phi-2)^2}{(\phi-1)^2} \right) \left(\frac{\rho}{2n+2} \right) \left[\left(\frac{\pi\tau_R}{t} \right)^{1/2} + \left(\frac{\pi\tau'_R}{t} \right)^{1/2} + \left(\frac{\pi\tau_{sb}}{t} \right)^{1/2} \exp\left(-\frac{2t}{\tau'_{sb}}\right) \right] \\
&\quad + \frac{(\phi-2)^2}{(\phi-1)^2} \frac{\rho}{2n+2} \left\{ \left(\frac{\pi\tau_R}{2t} \right)^{1/2} + \exp\left(-\frac{2t}{\tau''_{sb}}\right) \right\} \tag{S.40}
\end{aligned}$$

Further written in a more concise form,

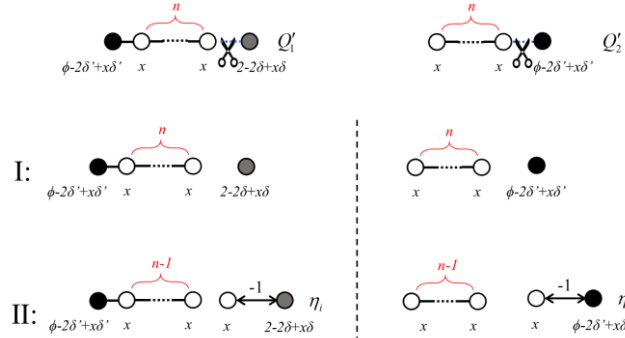
$$\begin{aligned}
G(\phi, t) &= \frac{1}{2\sqrt{2}} \left(1 - \frac{(\phi-2)^2}{(\phi-1)^2} \right) \left(\frac{\rho}{2n+2} \right) \left[\left(\frac{\pi\tau_R}{t} \right)^{1/2} + \left(\frac{\pi\tau'_R}{t} \right)^{1/2} + \left(\frac{\pi\tau_{sb}}{t} \right)^{1/2} \exp\left(-\frac{2t}{\tau'_{sb}}\right) \right] \\
&\quad + \frac{(\phi-2)^2}{(\phi-1)^2} \frac{\rho}{2n+2} \left\{ \left(\frac{\pi\tau_R}{2t} \right)^{1/2} + \exp\left(-\frac{2t}{\tau''_{sb}}\right) \right\} \tag{S.41}
\end{aligned}$$

$$\begin{aligned}
|RZ_{\text{matrix}} - \lambda \mathbf{1}|_{x=2-\lambda} &= \begin{vmatrix} x & -1 & 0 \\ -1 & x & -1 \\ & \dots & \\ & & -1 & x & -1 \\ 0 & & & & x \end{vmatrix} \xleftrightarrow{\text{Mapping}} \begin{array}{c} p_n(x) \\ \text{---} \\ \bigcirc \text{---} \dots \text{---} \bigcirc \\ x \quad x \quad \quad \quad x \quad x \end{array} \\
|RZ_{\text{matrix}} - \lambda \mathbf{1}|_{x=2-\lambda} &= \begin{vmatrix} x-1 & -1 & 0 \\ -1 & x & -1 \\ & \dots & \\ & & -1 & x & -1 \\ 0 & & & & x \end{vmatrix} \xleftrightarrow{\text{Mapping}} \begin{array}{c} \hat{p}_n(x) \\ \text{---} \\ \bigcirc \text{---} \dots \text{---} \bigcirc \\ x-1 \quad x \quad \quad \quad x \quad x \end{array}
\end{aligned}$$

(a)



(b)



(c)

Figure S1. Physical pictures of graph theory for dual network model based on affine network. (a) Mapping relations between the two basic RZ matrix (left column) and graph representation of RZ matrix eigen polynomials (Tshebyshev). (b) The cutting operation of graph theory, which is essentially the matrix reduction. (c) the further cutting operation for Q_1' and Q_2' subgraphs. The effective friction coefficient of two end segments $\delta' = \infty$,

represented by the solid black bead. The sticker with finite friction coefficient δ is shown as a gray solid bead, which divides the linear chains into two parts. The open bead is normal segment, and all bonds in this model have the same weighting factor $\eta = -1$. ϕ is the functional degree of networks, which will change the weighting factors of segments.

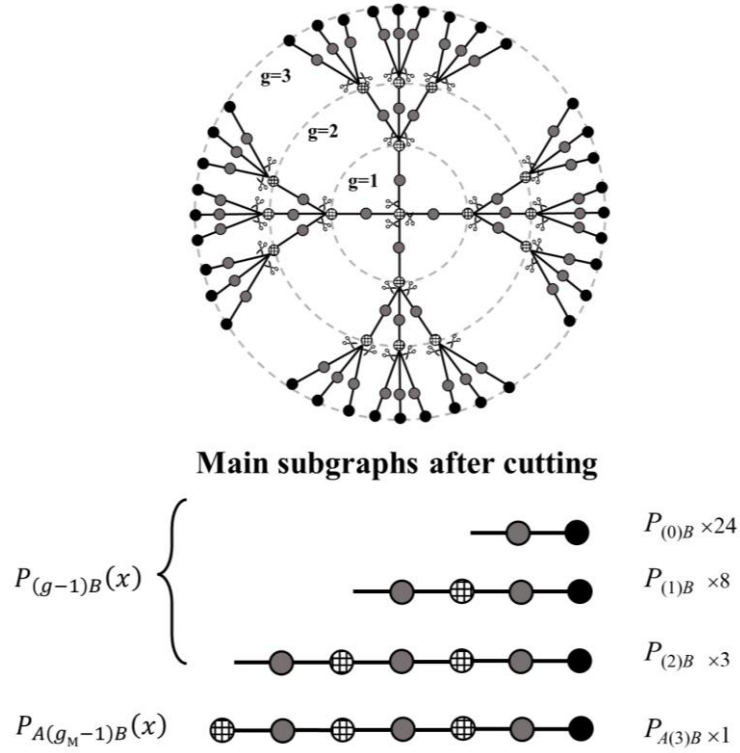


Figure S2. Main subgraphs obtained after successive rotational operations applied to our dual polymer networks model ($g = 3$ and $\phi = 4$), and all subgraphs can be divided into two categories, $P_{A(g_{\max}-1)B}(x)$ and $P_{(g-1)B}(x)$.

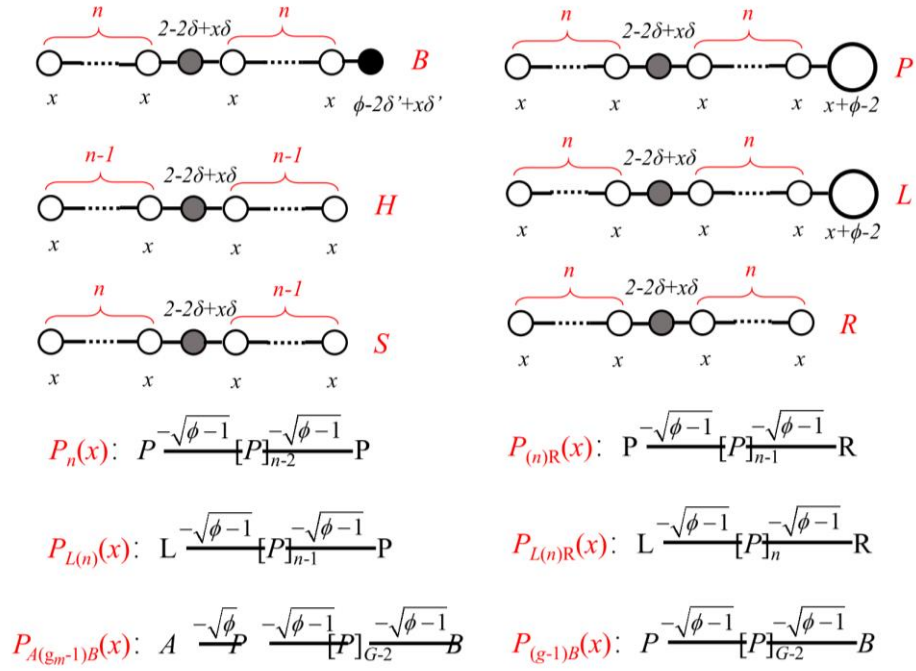


Figure S3. Subgraphs with linear structures are obtained following Theorem IV, which can be classified into six main basic subgraphs (B , H , S , P , L and R), four general subgraphs ($P_n(x)$, $P_{(n)R}(x)$, $P_{L(n)}(x)$ and $P_{L(n)R}(x)$) and two categories subgraphs ($P_{A(g_{\max}-1)B}(x)$ and $P_{(g-1)B}(x)$). The general subgraph is the function of six main basic subgraphs, and their weighting factors of the bonds and the beads has been marked.

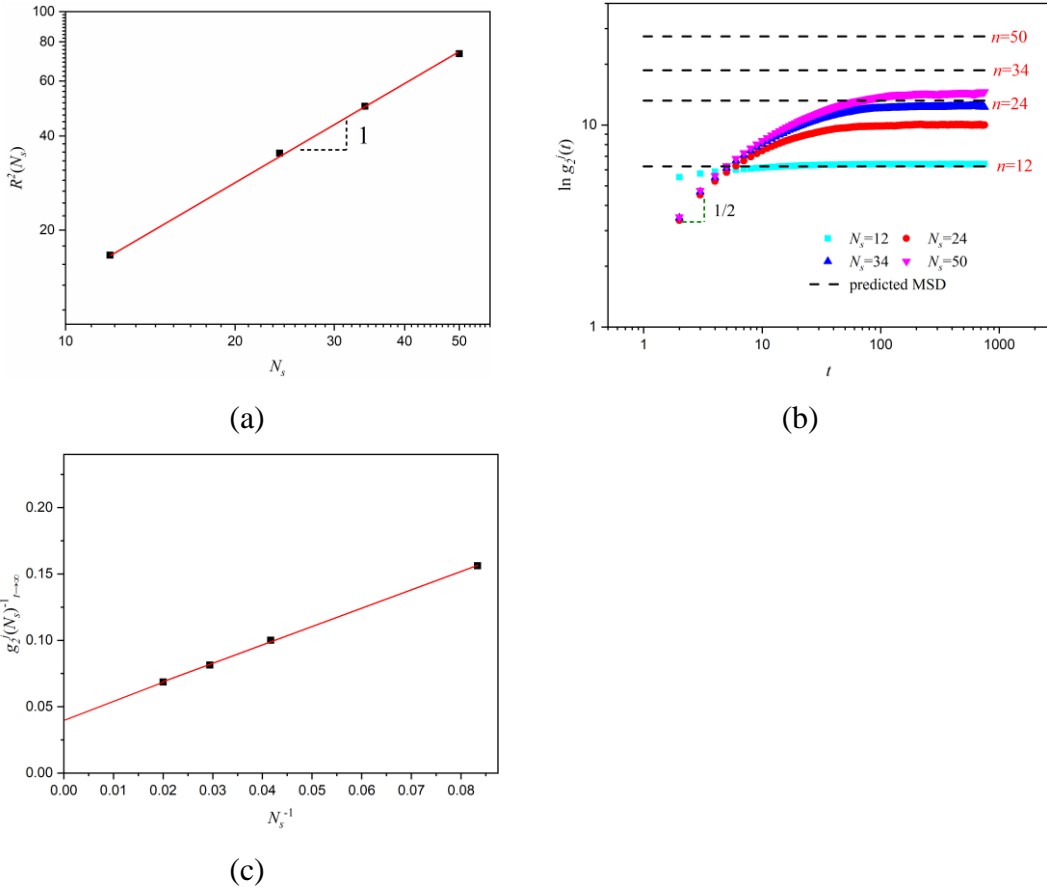


Figure S4. The strand size and MSD for junctions in the network. (a) The average mean square end-to-end distance of strands against the strand length N_s . (b) MSD of junctions under different strand length and the prediction of its maximum MSD. (c) MSD of junctions against the inverse of strand length N_s^{-1} . All simulation results are performed six times and then averaged.

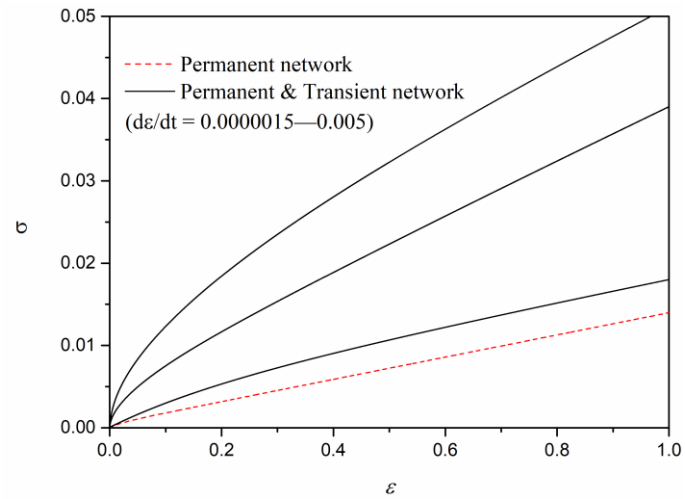


Figure S5. The stress–strain curves of small deformation with strain rates ranging from $1.5 \times 10^{-7} s^{-1}$ to $5 \times 10^{-3} s^{-1}$, where $n = 20$, $\delta = 1000$, $g = 10$ and $\phi = 4$. The result from permanent network is nearly linear and drawn out by a red dotted line.

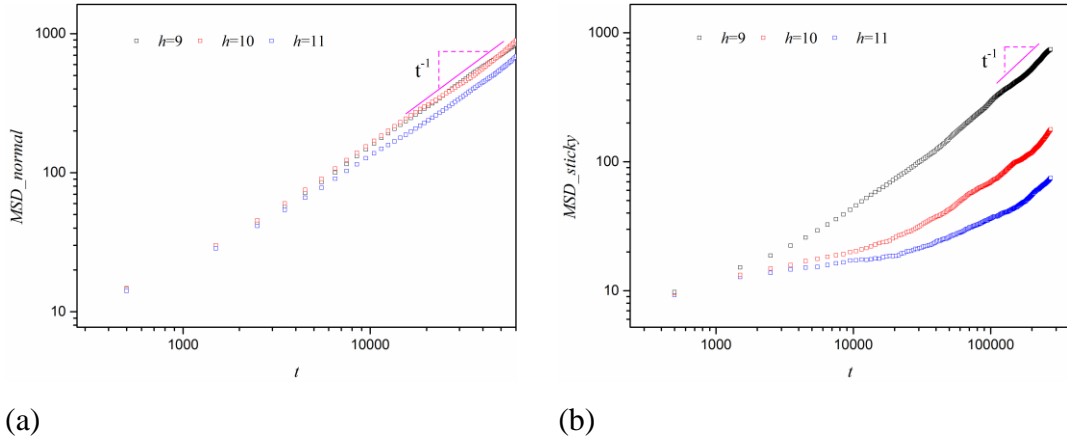


Figure S6. (a) MSDs of normal tracer chains. (b) MSDs of sticky tracer chains.

Table S1. Linear relaxation modulus and the trapping contribution from entanglements with strand length N_s from 12 to 50.

Modulus/ (ε/σ^3)	$N_s = 12$	$N_s = 24$	$N_s = 34$	$N_s = 50$
Phantom network model	0.035	0.018	0.013	0.009
Affine network model	0.071	0.035	0.025	0.017
Modified SRM	0.044	0.023	0.016	0.011
MD simulations	0.045	0.038	0.041	0.026
Trapping contribution $T_e G_N^0$	-	0.003	0.016	0.009

REFERENCE

1. Yang, Y. Graph Theory of Viscoelastic and Configurational Properties of Gaussian Chains. *Macromol. Theory Simul.* **1998**, 7 (5), 521-549.
2. Yang, Y.; Yu, T. Graph-Theory of Configurational and Viscoelastic Properties of Polymers .2. Linear Polymer-Chains Containing Small Copolymer Blocks. *Macromol. Chem. Phys.* **1986**, 187 (2), 441-454.
3. Yang, Y.; Qiu, F.; Zhang, H.; Yang, Y. The Rouse Dynamic Properties of Dendritic Chains: A Graph Theoretical Method. *Macromolecules* **2017**, 50 (10), 4007-4021.
4. Kloczkowski, A.; Mark, J. E.; Erman, B. Chain Dimensions and Fluctuations in Random Elastomeric Networks. 1. Phantom Gaussian Networks in the Undeformed State. *Macromolecules* **1989**, 22 (3), 1423-1432.
5. Kremer, K.; Grest, G. S. Dynamics of Entangled Linear Polymer Melts: A Molecular-Dynamics Simulation. *J. Chem. Phys.* **1990**, 92 (8), 5057-5086.
6. Vilgis, T.; Boue, F. Deformation Dependence of the Form-Factor of a Cross-Linked Chain in a Rubber - Entanglement and Orientational Effect. *Polymer* **1986**, 27 (8), 1154-1162.
7. Duering, E. R.; Kremer, K.; Grest, G. S. Structure and Relaxation of End-Linked Polymer Networks. *J. Chem. Phys.* **1994**, 101 (9), 8169-8192.